HHS Public Access

Author manuscript

Biomaterials. Author manuscript; available in PMC 2017 January 01.

Published in final edited form as:

Biomaterials. 2016 January ; 75: 123–134. doi:10.1016/j.biomaterials.2015.10.017.

3D brown adipogenesis to create "Brown-Fat-in-Microstrands"

Andrea M. Unser[1], **Bridget Mooney**[1], **David T. Corr**[2], **Yu-Hua Tseng**[3], and **Yubing Xie**[1,*]

[1]Colleges of Nanoscale Science and Engineering, SUNY Polytechnic Institute, 257 Fuller Road, Albany, NY 12203, USA

[2]Department of Biomedical Engineering, Rensselaer Polytechnic Institute, 110 8th Street, Troy, NY 12180, USA

[3]Section on Integrative Physiology and Metabolism, Joslin Diabetes Center, Harvard Medical School, Boston, MA 02215, USA

Abstract

The ability of brown adipocytes (fat cells) to dissipate energy as heat shows great promise for the treatment of obesity and other metabolic disorders. Employing pluripotent stem cells, with an emphasis on directed differentiation, may overcome many issues currently associated with primary fat cell cultures. In addition, three-dimensional (3D) cell culture systems are needed to better understand the role of brown adipocytes in energy balance and treating obesity. To address this need, we created 3D "Brown-Fat-in-Microstrands" by microfluidic synthesis of alginate hydrogel microstrands that encapsulated cells and directly induced cell differentiation into brown adipocytes, using mouse embryonic stem cells (ESCs) as a model of pluripotent stem cells, and brown preadipocytes as a positive control. Brown adipocyte differentiation within microstrands was confirmed by immunocytochemistry and qPCR analysis of the expression of the brown adipocyte-defining marker uncoupling protein 1 (UCP1), as well as other general adipocyte markers. Cells within microstrands were responsive to a β-adrenergic agonist with an increase in gene expression of thermogenic UCP1, indicating that these "Brown-Fat-in-Micrtostrands" are functional. The ability to create "Brown-Fat-in-Microstrands" from pluripotent stem cells opens up a new arena to understanding brown adipogenesis and its implications in obesity and metabolic disorders.

Keywords

Brown Fat; Adipocyte; Alginate; Hydrogel; Stem Cell; Adipose Tissue Engineering

[*]Corresponding author. Yubing Xie, Ph.D., Associate Professor, Colleges of Nanoscale Science and Engineering, SUNY Polytechnic Institute, 257 Fuller Road, Albany, NY 12203, Phone: (518) 956-7381, Fax: (518) 956-8687, YXie@sunycnse.com.

1. Introduction

The thermogenic capacity of brown adipose tissue (BAT) has changed the general conception of fat [1,2]. Originally, BAT remained “under the radar”, as it was primarily associated with rodents, hibernating animals, and human infants where activated BAT is responsible for nonshivering thermogenesis during cold exposure [3] and diet-induced thermogenesis [4,5]. However, BAT has become redefined by the recent confirmation of its existence and physiological significance in human adults [6–14]. This rediscovery has led to an influx of research concerning the role of BAT on the regulation of metabolic thermogenesis and thereby body fat content and triglyceride clearance [15,16]. Moreover, it is the innate ability of BAT that generates heat via a tightly controlled and extremely energy-expensive process. As a result, BAT provides an enormous impact on energy balance, which presents a clear therapeutic target, especially for treating obesity and related metabolic disorders, such as type 2 diabetes and non-alcohol hepatic steatosis [17–20].

The main cause of obesity, and thus obesity-related disease, is an energy imbalance in which energy intake exceeds energy dissipation [6,17,18]. Thus, it is critical to understand adipocyte biology for the development of potential obesity treatment strategies. During the development of obesity, adipocytes can increase in size (hypertrophy) or in amount (hyperplasia) [21,22]. Both cell conditions are known to occur in adolescents. However, adipocyte turnover is maintained at a steady state in adults [22]. The two main types of adipose tissue are white and brown adipose tissue [23]. White adipose tissue (WAT) is composed of unilocular white adipocytes, functions to store energy in the form of triglycerides, and acts as a vital endocrine and immune organ [24–27]. On the contrary, BAT is composed of multilocular brown adipocytes containing abundant mitochondria, and is specialized to expend energy as heat by uncoupling the synthesis of ATP from the electron transport chain with its unique mitochondrial membrane embedded protein, uncoupling protein 1 (UCP1) [24,28–32]. A new type of thermogenic adipocytes, known as beige, brite (brown in white), or inducible brown adipocytes, have been recently identified within white fat depots, named as such because they can be induced into brown-like adipocytes [9,33–38], thereby representing the plasticity of adipocytes [39]. Brown and beige fat can be activated by stimulation through cold exposure, receptor activation, exercise, hormone treatment (e.g., irisin, FGF21) or microRNA networks [40–54]. Similar to BAT, beige adipocytes express UCP1 and possess thermogenic capacity upon induction [18,36,55,56].

Although there is great potential for BAT to correct the energy imbalance in obese individuals, there are still many challenges to overcome prior to clinical applications. These include the need for an adequate cellular model system of human adipose tissue, as well as an effective implantation method. Although primary culture and differentiation of human adipocyte precursors have been used to understand adipocyte biology, these cells are difficult to obtain, culture, and expand *in vitro* [1], and fail to fully recapitulate human adipocyte development [57] and metabolic processes [58]. Pluripotent stem cells, including embryonic stem cells (ESCs) and induced pluripotent stem cells, provide a good model system for understanding early events in development [59–61] as well as an unlimited source of white, brown, and beige adipocytes [25,62–64]. The feasibility of generating brown or white adipocytes from human pluripotent stem cells has been demonstrated with

up to 85–90% differentiation efficiency through cellular programming and transplantation techniques [25,58]. However, this approach includes multiple steps and relies on transferring exogenous genes to derive adipocytes from pluripotent stem cells. For instance, human pluripotent stem cells are first differentiated into mesenchymal progenitor cells through embryoid body (EB) formation, followed by replating of EBs on gelatin-coated tissue culture dishes. Then, these mesenchymal progenitor cells are replated again and transduced with a lentivirus constitutively expressing the regulator genes of white or brown adipogenesis, respectively, followed by the addition of adipogenic factors such as insulin, dexamethasone, and rosiglitazone. In order to differentiate human pluripotent stem cells into functional, classic brown adipocytes without gene transfer, a specific hematopoietic cytokine cocktail has been used [63,65]. Differentiation in this manner also includes the formation of EB-like spheres as the very first step, and replating of these spheres on gelatin-coated tissue culture plates thereafter. Taken together, data from these techniques suggest that it would be beneficial to recreate a three-dimensional (3D) microenvironment for pluripotent stem cell differentiation and adipogenesis *in vitro* [66], including BAT formation. Additionally, although BAT transplantation has been demonstrated for decades [67], cell necrosis often occurs upon transplantation of free fat, resulting in poor formation of microvascular networks and graft resorption [68,69]. Altogether, there is a great need for a 3D culture system that could recreate the microenvironment for BAT differentiation from pluripotent stem cells, recapitulating BAT function during *in vitro* culture, and provide a new vehicle to improve the stability and engraftment efficiency during *in vivo* BAT transplantation.

We envision that cell encapsulation in alginate hydrogel microstrands could offer an effective 3D culture solution to address the needs for BAT differentiation and transplantation. Alginate is an FDA-approved biomaterial that has been demonstrated to be safe for drug delivery, stem cell culture, tissue engineering, and cell therapy [70–73]. The long tubular structure and small diameter (200 μm) of alginate hydrogel microstrands can easily overcome the diffusion limitation that challenges the use of hydrogel microbeads for cell implantation [74], which allows for more efficient signaling, nutrient and oxygen exchanges, and support for high cellularity of stem cells grown in the tubular structure [75,76]. Additionally, these microstrands are easy to be handled for *in vivo* delivery by injection or implantation while maintaining their structural integrity. Moreover, alginate hydrogel microstrands exhibit great potential for reconstituting intrinsic morphologies and functions of living tissues [77,78]. The current approaches to fabricate hydrogel microstrands include utilizing coaxial flow and a microfluidic chip [79], flowing through a microfabricated SU-8 filter by a variety of techniques, including capillary force [75,76], wet spinning [80], composite techniques [81]. Here, we present a new microfluidic approach for cell encapsulation in alginate hydrogel microstrands, by simply driving an alginate solution to flow consistently into a calcium solution.

In this study, we create “Brown-Fat-in-Microstrands” by encapsulating brown preadipocytes and pluripotent stem cells in 3D alginate hydrogel microstrands, and directly differentiating them into functional brown adipocytes. Mouse embryonic stem cells (ESCs) are used as model of pluripotent stem cells to test the feasibility of 3D brown adipogenesis in alginate

microstrands. Mouse WT-1 brown preadipocytes are also grown within the same system to serve as a positive control. We culture cells within the alginate hydrogel microstrand system, and then expose them to a brown adipogenic differentiation scheme. We then assess the expression of characteristic brown adipogenesis markers, compare to 2D differentiation, and test for functional responsiveness. This bioengineered "Brown-Fat-in-Microstrands" has great potential to serve as an *in vitro* culture system for understanding brown adipogenesis, an *in vitro* assay for testing the efficacy of treatment, and as a stable, functional brown fat depot for *in vivo* implantation.

2. Materials and Methods

2.1 ES cell culture

The mouse CCE ES cell line was provided by StemCell Technologies, Inc. (Vancouver, Canada) [82,83]. Cells were cultivated in gelatin-coated tissue culture flasks and maintained in an undifferentiated state using maintenance medium. This maintenance medium consisted of Dulbecco's Modified Eagle's Medium (DMEM 4.5 g/l D-glucose), enhanced with 15% (v/v) fetal bovine serum (FBS), 10 ng/ml murine recombinant leukemia inhibitory factor (LIF; StemCell Technologies), 0.1 mM non-essential amino acids, 0.1 mM monothioglycerol, 100 U/ml penicillin, 100 μg/ml streptomycin, and 2 mM L-glutamine, and 1 mM sodium pyruvate (Sigma-Aldrich, St Louis, MO).

2.2 WT-1 preadipocyte culture

Murine WT-1 preadipocyte line was provided by Dr. Yu-Hua Tseng (Joslin Diabetes Center, Harvard Medical School Affiliate, Boston, MA). The cells were cultured following a previously established protocol [84,85]. Briefly, WT-1 preadipocytes were propagated in DMEM supplemented with 10% FBS and 1% penicillin-streptomycin. When the cells were ready to be split for experimentation, 0.1 μg/mL insulin and 10^{-8} μM T3 were added to the maintenance medium to begin the differentiation process on day 1 (this medium will be referred to as differentiation medium). To induce differentiation into brown adipocytes, at 4-day postconfluence, cells were treated with DMEM containing 10% FBS, 125 μM indomethacin, 1 μM dexamethasone, 0.5 mM 3-isobutyl-1-methylxanthine, 0.1 μg/ml insulin, and 10^{-8} μM triiodothyronine (T3) (Sigma-Aldrich). The cells were incubated in this induction medium for day 5, and then refed with the differentiation medium on days 6 and 8 to be ready for characterization by day 10.

2.3 Fabrication of alginate microstrands containing ESC and WT-1 cells

One million mouse ESCs were suspended in 1 mL of 1.5% alginate (made from sodium alginate from brown algae with a viscosity of 100–300 cP in 2% solution at 25 °C, Sigma-Aldrich) in physiological saline solution at 37°C. This ESC-alginate suspension was then loaded into a syringe in a pump set to dispense 0.5 mL/hr. A capillary silica tip (diameter of 100–250 μm) was then attached to the end of the syringe via an adapter. The pump was then inverted so that the tip was downward facing, and then allowed to dispense for 1–5 minutes to calibrate. Dispensing without interruption was continued following calibration, with the tip being shaken to remove any possible alginate build-up, and then inserted into the calcium chloride solution (Sigma-Aldrich) within the well of a 24-well plate (Fig. 1). The timer was

then set to 1–5 minutes, with constant shaking of the tip to prevent obstruction. After the first well was completed, the microstrands were imaged using an inverted microscope (Nikon Eclipse TS100) in order to confirm proper formation. After confirmation, the process was repeated for several more wells in order to obtain a sufficient number of microstrand samples. The gel core microstrands were simply formed by removing the extra calcium chloride solution after fabrication and adding the proper cell media to facilitate growth. The liquid core microstrands were formed by coating the alginate hydrogel microstrands with 0.05% poly-L-lysine (PLL) (Sigma-Aldrich) by constant rocking for 10 minutes, and then incubating with 1.6% sodium citrate (Sigma-Aldrich) for 3 minutes in order to sequester the alginate inside the alginate-PLL shell. The liquid core microstrands were then placed in the proper cell media to facilitate cell growth.

WT-1 preadipocytes were subcultured as usual, and resuspended in the same fashion as the ESCs. The only difference was that the WT-1 preadipocytes were suspended at three times the density of the ESCs within the alginate (3×10^6 cells/mL). Characterization was extended past day 10 so that the WT-1 preadipocytes had sufficient time to grow and differentiate within the alginate microstrands.

2.4 Differentiation scheme of mESCs into brown adipocytes to create “Brown-Fat-in-Microstrands”

After the cells were encapsulated within the microstrands, they were incubated with cultivation medium (Iscove’s Modified Dulbecco’s Medium, 2 mM L-glutamine, 0.1 mM MEMs amino acids, 10% heat inactivated FBS, and 100 μM β-mercaptoethanol, (FBS is from Fisher Scientific, all other materials from Sigma-Aldrich) for the first two days. After this initial incubation, the untreated control group remained in cultivation medium whereas the differentiation group was treated with 10^{-8} M retinoic acid (RA) (Sigma-Aldrich) for 4 days. After a day of rest, the ESC-hydrogel microstrands were exposed to 3.3 nM BMP7 for 4 days. At this point, the cells should be at the brown preadipocyte stage, and were then induced into brown adipocytes using Adipocyte Induction Medium (cultivation medium supplemented with 5 μM dexamethasone, 125 μM indomethacin, 0.5 mM 3-isobutyl-1-methylxanthine (IBMX), 1 nM T3, and 20 nM insulin) (Sigma-Aldrich) for 3 days. In order to ensure the maturity of the brown adipocytes, they were maintained in differentiation medium (cultivation medium supplemented with 1 nM T3 and 20 nM insulin) with regular changing of the differentiation medium every 2 days. After 4 weeks “Brown-Fat-in-Microstrands” were established.

2.5 Oil Red O staining

A working solution of oil red O (Sigma-Aldrich) was prepared by mixing the stock solution (15 mg of oil red O dissolved for 1–2 hours in 50 mL of 99% isopropanol (Fisher Scientific, Waltham, MA)) in distilled water in a ratio of 6 parts stock to 4 parts water.

Both the control and differentiation group cells-in-microstrands were washed with physiological saline and then stained in the working solution of oil red O for 6–15 minutes. The background was then cleared with 60% isopropanol and the cells-in microstrands were

washed a second time in physiological saline and imaged using a brightfield microscope (Nikon Eclipse TS100).

2.6 Immunocytochemistry analysis of brown and adipocyte-defining markers

In order to determine if the mouse ESCs have properly differentiated into brown adipocytes, immunocytochemistry analysis of UCP1 (brown adipocyte-defining marker), perilipin (surface marker of adipocytes) and PPARγ2 (adipocyte transcription factor) was performed. Mouse ESCs within the alginate microstrands were fixed using a 4% paraformaldehyde solution (Sigma-Aldrich), permeabilized using 0.2% Triton-X 100 (Sigma-Aldrich) in physiological saline, and blocked using 5% FBS in physiological saline (StemCell Technologies). Samples were incubated with the primary antibodies of perilipin (Santa Cruz Biotechnology, Inc., Dallas, Texas), PPARγ2 (Santa Cruz Biotechnology, Inc.), and brown adipocyte-defining UCP-1 (Santa Cruz Biotechnology, Inc.), at 4°C overnight or room temperature for 1 hour. The immunoreactivities were detected using secondary antibodies Alexa Fluor® 488 (perilipin) and Alexa Fluor® 647 (PPARγ2 or UCP1). Total cell population was revealed by staining cell nuclei with DAPI. All samples were imaged using the Leica Sp5 confocal microscope (Leica Microsystems, Wetzlar, Germany).

2.7 Quantitative Polymerase Chain Reaction

RNA was harvested from the samples using a combination of TRIzol® homogenization and chloroform phase separation (Life Technologies, Carlsbad, CA) followed by isolation using an RNeasy kit (Qiagen, Valencia, CA). The RNA samples were then reverse transcribed using a first-strand cDNA synthesis kit (Invitrogen, Grand Island, NY).

Quantitative real-time PCR (qPCR) analysis was performed using a StepOnePlus™ Real Time PCR system (Applied Biosystems, Foster City, CA). Samples were amplified using a SYBR® green I PCR master mix. Reactions were analyzed in triplicate and expression levels were normalized to the housekeeping gene ARBP. The relative quantitation of UCP1 in addition to a transcriptional regulator highly expressed in brown adipose tissue, PRDM16, and an adipocyte protein, aP2, were also determined using the comparative Ct method.

2.8 Functional analysis of “Brown-Fat-in-Microstrands”

In order to determine whether bioengineered “Brown-fat-in-Microstrands” were functional, responsiveness to the β-adrenergic agonist, isoproterenol (Sigma-Aldrich), was assessed. Briefly, 10 μM isoproterenol in cultivation medium was added to the “Brown-fat-in-Microtrands” and incubated at 37°C for 5 hours. Samples were then washed three times in 0.9% sodium chloride and further characterized by qPCR analysis for the brown adipogenic gene UCP1.

2.9 Statistical analysis

Data for qPCR analysis are presented as mean with standard deviation. Two-tailed Student’s t-test was used to determine p values. Statistical significance was defined as $p<0.05$.

3. Results

3.1 3D adipogenesis of WT-1 preadipocytes within alginate hydrogel microstrands

To demonstrate the feasibility of 3D adipogenesis, we have developed the microfluidic synthesis of alginate hydrogel microstrands (Fig. 1), followed by coating with poly-L-lysine to form a semipermeable membrane and then liquefying the gelled core with sodium citrate. In this way, WT-1 preadipocytes were successfully encapsulated in liquid core alginate microstrands with a diameter of 200 μm, induced to undergo brown adipogenesis, and cultured for 20 days.

Cells propagated in alginate microstrands, and maintained a dense cell mass after 11 days of cultivation, as observed under an optical microscope (Fig. 2a–f), which showed similar morphology to the undifferentiated sample set (data not shown). Adipogenic differentiation of WT-1 preadipocytes in alginate microstrands was initially confirmed by positive oil red O staining to show lipid accumulation in red (Fig. 2g) while the control group did not show positive oil red O staining (Fig. 2h).

To determine that differentiated WT-1 cells in alginate microstrands become brown fat cells, we have examined the expression of adipocyte markers (PPARγ2, perilipin), and a brown adipocyte marker (UCP1), using immunocytochemistry (Fig. 3). Alginate hydrogel microstrands containing differentiated WT-1 cells on day 15 stained positively for adipocyte transcription factor PPARγ2 (Fig. 3a), adipocyte surface marker perilipin (Fig. 3b and e), and brown adipocyte marker UCP-1 (Fig. 3d), indicating that differentiated WT-1 cells in alginate microstrands acquire a brown adipocyte phenotype. Negative immunocytochemistry control for each secondary antibody was performed and showed no immunoreactivity, confirming that the immunoreactivity observed in differentiated samples was true (Fig. 3g–i). Additionally, brown WT-1 preadipocytes not exposed to the aforementioned differentiation scheme were used as undifferentiated control, showing no expression of adipocyte markers of PPARγ2 or perilipin, or brown adipocyte marker UCP-1. (Fig. 3j–o). Although present, the weak level of expression inspired the extension of the WT-1 differentiation timeline to day 20 (Fig. 2f) within alginate microstrands in order to ensure maturation of the brown adipocytes.

To further confirm the terminal differentiation of WT-1 cells into brown adipocytes within alginate microstrands beyond day 15, we quantified the expression of brown adipocyte genes (UCP1 and PRDM16) along with adipocyte genes (PPARγ2, PGC1α, and aP2) using qPCR. Both brown adipocyte genes UCP1 and PRDM16, as well as the adipocyte gene (aP2), were expressed at relatively higher levels in differentiated WT-1 cells within alginate microstrands (3D WT1 T) than in those of the control group, grown in 3D microstrands without brown adipogenic induction (3D WT1 C) (Fig. 4). However, PPARγ2 and PGC1α were both expressed relatively lower in the 3D WT1 T than the 3D WT1 C samples. It is interesting to notice that the expression of PPARγ2 of brown adipocyte-differentiated WT-1 cells in alginate microstrands is higher than the undifferentiated control at protein level, but lower than that at mRNA level. These cumulative data demonstrate that WT-1 preadipocytes can grow and differentiate into characteristic brown adipocytes in alginate microstrands three dimensionally.

3.2 Direct differentiation of mouse ESCs within alginate hydrogel microstrands and creation of "Brown-Fat-in-Microstrands"

Next, we have developed a differentiation scheme to induce mouse ESCs in hydrogel microstrands directly into brown fat cells. Mouse ESCs were successfully encapsulated in alginate hydrogel microstrands. Our strategy to differentiate ESCs into brown fat cells includes i) driving ESCs to a mesenchymal stem cell (MSC)-like lineage by retinoic acid (RA) treatment, ii) deriving brown preadipocyte-like cells from MSCs by BMP-7 treatment, and iii) further inducing brown adipogenesis using brown adipocyte induction cocktails (Fig. 5a).

Critical parameters of the microstrands were investigated to determine how microstrands should be created to optimize brown adipogenesis of mouse ESCs. In brown adipocytes, a dense cell mass formation is necessary because of the requirement of a high density of preadipocytes prior to induction. The first parameter explored was the interior environment; a liquid interior vs. a gel core, to determine which better produced the desired dense cell growth. Microstrands with a liquid core dramatically facilitated high-density cell growth, which is essential for adipogenesis induction (Fig. 5b), while those with gel core retained ESCs as small cell aggregates (Fig. 5c). Because adipose tissue is a dense tissue, it was important for the cells to have the ability to aggregate and form a dense cluster. In particular, contact inhibition when cells reach a high density is generally a prerequisite for the differentiation of preadipocytes. Therefore, microstrands with a liquid core were chosen for brown adipogenesis. In terms of the different microstrand diameters, both facilitated the growth of ESCs within microstrands into high-density colonies.

The second parameter tested was the diameter of the silica capillary tip. The tip diameters that were tested were 100–250 μm. Considering that the transport of oxygen, nutrients, and metabolic waste by diffusion becomes limited when the diffusion distance is over 200 μm [86,87], we chose to fabricate microstrands using a tip within the 100–200 μm range (compare Fig. 5d to 5e) for future experiments.

Finally, the concentration of bone morphogenetic protein 7 (BMP7) (R&D Systems Inc., Minneapolis, MN) was also explored. BMP7 is an essential component in the differentiation scheme presented in this work. The two concentrations tested were 3.3 and 8.3 nM. BMP7 plays an important role in stem cell differentiation to brown fat cells [88]. The decision between the concentrations of 3.3 and 8.3 nM BMP7 was expected to be easily determined by differences in lipid accumulation, qualitatively observed by oil red O staining. However, there was not a major difference between the two BMP7 concentrations (Fig. 5f and g). It has been reported that BMP7 at higher concentration might favor osteogenesis [89–91]. Therefore, we decided to pursue 3.3 nM BMP7 for future experiments.

Based on our aforementioned pilot studies, we have encapsulated mouse ESCs in liquid core alginate hydrogel microstrands with a diameter less than 200 μm, followed by differentiation as scheduled in Fig. 5a with 3.3 nM BMP7. The time course of mouse ESCs grown within hydrogel microstrands during brown fat differentiation is shown in Fig. 5h–m. ESCs formed cell colonies in microstrands before day 3, and the aggregates of ESC colonies elongated with time, suggesting that the differentiation treatment did not affect cell growth. After 20

days of cultivation, differentiating ESCs tended to fully occupy the space in hydrogel microstrands, and exhibited lipid droplet accumulation as shown by oil red O staining at day 27 (Fig. 5n).

We have confirmed that these differentiated ESCs in hydrogel microstrands expressed brown adipocyte-defining marker UCP1 along with general adipocyte markers using immunocytochemistry and qPCR analysis (Fig. 6a–i and Table 1). The expression of adipocyte transcription factor PPARγ2 (Fig. 6a), adipocyte surface marker perilipin (Fig. 6b and e) and, in particular, brown adipocyte defining marker UCP1 (Fig. 6d) at the protein level indicated brown adipogenesis occurred.

The quantitative expression of brown adipocyte gene, UCP1 as well as PRDM16, and aP2 was determined using qPCR. As shown in Table 1, the control group of mouse ESCs in microstrands without any induction of brown adipogenesis (3D CCE C) did not have any detectable expression of brown adipocyte genes. Directly-differentiated ESCs within hydrogel microstrands (3D CCE T) showed high levels of the brown adipocyte-defining gene UCP1 and PRDM16, indicating the formation of “Brown-Fat-in-Microstrands”.

3.3 Comparison of 3D and 2D adipogenesis

To compare the degree of differentiation in our “Brown-Fat-in-Microstrands” to brown adipocyte differentiation of cells under monolayer conditions, we also differentiated mouse ESCs grown on glass (2D CCE T) using the differentiation scheme as shown in Fig. 5a. Brown adipocyte-defining marker UCP1 as well as PPARγ2, PGC1α, PRDM16 and aP2 were relatively expressed at higher levels than the undifferentiated ESCs (2D CCE C) (Fig. 7a), indicating that our differentiation scheme can drive ESCs grown on 2D into brown fat cells as well. When comparing 2D and 3D brown adipocyte-differentiated ESCs, we have noticed that 3D differentiated ESCs (3D CCE T) exhibited a significantly higher relative expression of UCP1, PGC1α and aP2 (Fig. 7b). It is this increased relative expression of UCP1 that is especially worth highlighting, as it is the only gene in this that defines brown adipogenesis. However, the 3D differentiated ESCs did not appear to express PPARγ2 and PRDM16 any differently when compared to the 2D differentiated ESCs. In addition, the decreased expression of PPARγ2 and PGC1α in 2D CCE T compared to 2D CCE C was similar to that of the 3D WT-1 brown preadipocytes discussed in Fig. 4. This could indicate that the long-term culture could be spontaneously differentiating the “control” into adipocytes. This was tested by examining the relative expression of UCP1, PPARγ2, PGC1α, PRDM16, and aP2 on long-term cultured 2D CCE C and ESCs grown only for 2 days (2D CCE Day 2) in which no spontaneous differentiation has occurred. In fact, Fig. 7c shows the significantly increased relative expression of PPARγ2 and aP2, both markers of adipocyte differentiation, for 2D CCE C compared to 2D CCE Day 2. In particular, PPARγ2 was dramatically increased up to 6600 fold change in 2D CCE C untreated long-term culture compared to undifferentiated 2-day ESC culture (2D CCE Day 2) (Fig.7c), indicating that expression of PPARγ2 in untreated 2D and 3D ES cells was a result of long-term ES cell culture itself. PRDM16 was also increased in 2D CCE C compared to 2D CCE Day 2, which reinforces its alternative role as a coactivator of PPARγ2. Notably, UCP1 did not exhibit this trend. These data indicate that long-term culture of ESCs could induce spontaneous

differentiation to adipocytes, but not UCP1-expressing brown adipocytes. Increased UCP1 expressions at protein and mRNA level in BMP7-induced, differentiated ESCs in alginate microstrands confirm that bioengineered “Brown-Fat-in-Microstrands” are exhibiting brown adipocyte characteristics.

3.4 Functional analysis of “Brown-Fat-in-Microstrands”

To examine whether bioengineered “Brown-fat-in-Microstrands” are functional, we evaluated their mitochondrial activity by measuring the oxygen consumption rate (OCR) using Seahorse XF Cell Mito Stress Test Kit. The “Brown-Fat-in-Microstrands” were responsive to Mito Stress challenges (Fig.S1). The calculation showed that maximal OCR of differentiated ESCs in hydrogel microstrands went up to 200 pmol/min, which was higher than undifferentiationed ESCs in microstrands (~100 pmol/min).

We further assessed their response to the well-known β-adrenergic agonist, isoproterenol. The treatment of directly differentiated ESCs within hydrogel microstrands with 10 μM isoproterenol showed the higher relative gene expression of brown adipocyte-defining thermogenic UCP1, when compared to the untreated control (Fig. 8).

4. Discussion

In recent years, significant efforts have been made to understand the biology of brown adipose tissue and its potential as a new therapeutic for obesity [92–94]. This could, in turn, treat a myriad of diseases caused by obesity, including type II diabetes and cardiovascular disease. However, there is an unmet need for a 3D brown adipocyte culture system that recapitulates the form and function of brown fat, both for *in vitro* assay development and for *in vivo* implantation.

To address this technical need, cell encapsulation and differentiation in alginate microstrands to create “Brown-Fat-in-Microstrands” has been established in this study, using mouse pluripotent ESC differentiation as a model system. The merit of this study lies in: 1) a new and very straightforward approach to microfluidic synthesis of alginate hydrogel microstrands for cell encapsulation; 2) 3D brown adipogenesis in alginate hydrogel microstrands; 3) direct differentiation of pluripotent stem cells into functional brown adipocytes without requiring gene transfer and/or multiple stages. The feasibility of adipogenic differentiation in alginate hydrogel microbeads has been demonstrated by human adipose-derived stromal cells, exhibiting increased lipid accumulation and adipocyte gene expression or high ratio of evenly distributed adipocytes [95,96]. In addition, ESCs encapsulated within alginate microbeads were differentiated to release insulin, and it was confirmed that 3D differentiation systems increased insulin production over that achieved in 2D systems [97]. Mouse ESCs have also been encapsulated in alginate-poly-L-lysine microcapsules and have been exposed to a differentiation scheme leading to functional hepatocytes [98]. Although the mouse ESCs have the ability to grow within the microbeads and microcapsules, the diameter is typically just outside of the 200-μm diffusion limit, and thus, oxygen and nutrients will not be transported to the center of the cell aggregates uniformly [99–103]. Therefore, it is beneficial to fabricate long microstrands with diameters

less than 200 μm, to overcome the diffusion limit and prevent necrotic regions in the center of cell aggregates [104] while still allowing for abundant cell growth.

This study is the first to show that cells encapsulated in alginate microstrands with a liquid core can be directed to differentiate into mature brown fat, as evidenced by the accumulation of lipid droplets, expression of the brown adipocyte-defining marker UCP1 at both the protein and mRNA levels, and responsiveness to the β-adrenergic agonist with increased thermogenic UCP1 gene expression. The significance and potential of cell-laden hydrogel microfibers has been documented by reconstructing muscles, blood vessels, neural networks, and pancreatic islets in alginate-based hydrogel microfibers [77,105,106] as well as long-term maintenance and cryopreservation of human pluripotent stem cells [78]. Previous work has created microstrands utilizing a variety of fabrication techniques [107–112]. One technique, in particular, encapsulated ESCs in alginate using an SU-8 filter and capillary action to create the microstrands. Mouse ESCs were cultured within the strands in both a liquid and gel interior microenvironment. The cells were shown to grow more freely and self-assemble into a high density cell mass within the liquid microenvironment, whereas cells within the gel system remained small aggregates [75]. Microstrands with an inner core of ECM proteins and a calcium-alginate hydrogel shell have also been produced using a double-coaxial laminar-flow microfluidic device [77]. These constructs allowed for effective morphology and functions including the contraction of primary myocytes and tubular shape of primary endothelial cells [77]. In this paper, we presented an efficient, straightforward microfluidic approach to cell encapsulation in alginate hydrogel microstrands by simply driving an alginate solution to flow consistently into a calcium solution.

Spontaneous differentiation of ESCs into adipocytes has been cited as a rare event [113]. However, one method that has been well established for ESCs to commit to an adipogenic lineage is to treat EBs with all-*trans*-retinoic acid (RA) [113,114]. The concentration for RA is critical, however, because high concentrations of RA can cause differentiation of cells into a neural lineage in combination with other neurogenic factors [115]. Therefore, we choose a relatively low concentration (10^{-8} M) of RA for initial induction. Human pluripotent stem cells have been programmed to differentiate into brown adipocytes by transducing cells with a lentiviral construct [25]. In that study, human pluripotent stem cells were first differentiated into mesenchymal progenitor cells (MPCs), and then transduced with combinations of doxycycline-inducible lentiviral constructs that encoded for the transcription factors PPARγ2, CEBPβ, and PRDM16. These transcription factors were chosen based upon previous work showing that PPARγ2 is a key regulator of adipogenesis [116], PRDM16 can convert mouse myoblasts into brown adipocytes [32], and a combination of CEBPβ and PRDM16 can convert mouse cells and human fibroblasts into brown adipocyte-like cells [29]. It was determined that any transcription factor combination that included PPARγ2 induced a greater expression of the brown adipocyte-defining marker UCP1 [25]. In addition, the human pluripotent stem cells-derived brown adipocytes were injected subcutaneously *in vivo* and analyzed after 4–6 weeks. The implanted cells stained positively for UCP1 expression. Moreover, fluorodeoxyglucose (^{18}FDG) uptake followed by positron-emission-tomography-computed tomography (PET-CT) showed that the transplanted hPSC-derived brown adipocytes had great ability to uptake FDG [25]. This is

consistent with the notion that brown adipocytes act as a ‘glucose sink’, in that these cells are able to uptake large quantities of glucose as contribution to their vast metabolic capacity [25]. These aforementioned studies demonstrated the feasibility of differentiating of pluripotent stem cells into functional brown adipocytes. However, their reliance on gene transfer and multiple steps calls for a simplified, non-gene delivery approach to brown adipogenesis of pluripotent stem cells.

In this study, we have established a direct 3D brown adipogenesis approach by combining the microfluidic sysnthesis of alginate hydrogel microstrands for cell encapsulation with a directed differentiation of pluripotent stem cells into brown adipocytes. We first used WT-1 preadipocytes as a positive control to ensure that alginate hydrogel microstrands support preadipocyte growth, propagation, and terminal differentiation into brown adipocytes. This confirmation was determined using immunocytochemistry and qPCR analysis of brown adipocyte markers including UCP1, a brown adipocyte protein [117,118]. A differentiation scheme was presented here based upon several studies of differentiation of ESCs into MSC-like lineage, and MSCs into mature brown adipocytes [66,88,119]. Our results showed that ESCs could grow, propagate, and even differentiate within the alginate hydrogel microstrands. Immunocytochemistry and qPCR results confirmed the expression of brown adipocyte markers including brown adipocyte-defining UCP1. Functional analysis confirmed the ESC-derived 3D “Brown-Fat-in-Microstrands” responded to the β-adrenergic agonist, isoproterenol to upregulate the gene expression of thermogenic UCP1, which demonstrates the feasibility of these constructs to exert thermogenic activity and serve as an *in vitro* drug-screening platform.

Furthermore, the degree of ESC differentiation within the 3D alginate hydrogel microstrands was compared to that in a traditional 2D system. A qPCR analysis showed that ESCs differentiated in 3D expressed UCP1, PRDM16, PGC1α and aP2 at higher levels than ESCs differentiated in 2D. This finding is consistent with literature reports that have shown 3D differentiation of pluripotent stem cells are more effective than 2D, by preferable representation of an *in vivo* system with improved scalability [66,76,120,121].

Altogether, this study demonstrates the feasibility of 3D adipogenesis of pluripotent stem cells to construct functional “Brown-Fat-in-Microstrands”, which has great potential for *in vitro* analyses and *in vivo* implantation.

5. Conclusions

Preadipocytes and ESCs can be successfully encapsulated, grown, and differentiated into brown adipocytes within 3D alginate hydrogel microstrands, forming “Brown-Fat-in-Microstrands” that express the brown adipocyte-defining marker UCP1 and exhibit characteristic brown adipocyte activation in response to β-adrenergic agonists. A higher level of gene expression of the brown adipocyte marker UCP1, in ESCs differentiated in 3D hydrogel microstrands than the traditional 2D culture system, indicated 3D adipogenesis is more efficient than 2D. Future work will explore using the ESC-differentiated “Brown-Fat-in-Microstrands” to understand early events during brown adipogenesis, to test potential obesity agents, and determine the feasibility of *in vivo* implantation.

Supplementary Material

Refer to Web version on PubMed Central for supplementary material.

Acknowledgements

This work was supported by NIH NIDDK 1R56DK088217, NSF DBI-0922830, and The Wendell Williams Memorial Fellowship for Excellence in Teaching and Mentoring (AMU). Additional thanks to Dr. Nadine Hempel for comments on the manuscript during preparation.

References

1. Peirce V, Carobbio S, Vidal-Puig A. The different shades of fat. Nature. 2014; 510:76–83. [PubMed: 24899307]
2. Owens B. Cell physiology: The changing colour of fat. Nature. 2014; 508:S52–S53. [PubMed: 24740126]
3. Selye H, Timiras PS. Participation of brown fat tissue in the alarm reaction. Nature. 1949; 164:745. [PubMed: 15391333]
4. Rothwell NJ, Stock MJ. A role for brown adipose tissue in diet-induced thermogenesis. Nature. 1979; 281:31–35. [PubMed: 551265]
5. Trayhurn P, Jones PM, McGuckin MM, Goodbody AE. Effects of overfeeding on energy balance and brown fat thermogenesis in obese (ob/ob) mice. Nature. 1982; 295:323–325. [PubMed: 7057896]
6. Cypess AM, Lehman S, Williams G, Tal I, Rodman D, Goldfine AB, et al. Identification and importance of brown adipose tissue in adult humans. N Engl J Med. 2009; 360:1509–1517. [PubMed: 19357406]
7. Van Marken Lichtenbelt WD, Vanhommerig JW, Smulders NM, Drossaerts JMaFL, Kemerink GJ, Bouvy ND, et al. Cold-activated brown adipose tissue in healthy men. N Engl J Med. 2009; 360:1500–1508. [PubMed: 19357405]
8. Virtanen KA, Lidell ME, Orava J, Heglind M, Westergren R, Niemi T, et al. Functional brown adipose tissue in healthy adults. N Engl J Med. 2009; 360:1518–1525. [PubMed: 19357407]
9. Nedergaard J, Bengtsson T, Cannon B. Unexpected evidence for active brown adipose tissue in adult humans. Am J Physiol Endocrinol Metab. 2007; 293:E444–E452. [PubMed: 17473055]
10. Lee P, Zhao JT, Swarbrick MM, Gracie G, Bova R, Greenfield JR, et al. High prevalence of brown adipose tissue in adult humans. J Clin Endocrinol Metab. 2011; 96:2450–2455. [PubMed: 21613352]
11. Yoneshiro T, Aita S, Matsushita M, Kameya T, Nakada K, Kawai Y, et al. Brown adipose tissue, whole-body energy expenditure, and thermogenesis in healthy adult men. 2011; 19
12. Yoneshiro T, Aita S, Matsushita M, Okamatsu-Ogura Y, Kameya T, Kawai Y, et al. Age-related decrease in cold-activated brown adipose tissue and accumulation of body fat in healthy humans. Obesity (Silver Spring). 2011; 19:1755–1760. [PubMed: 21566561]
13. Ouellet V, Labbé SM, Blondin DP, Phoenix S, Guérin B, Haman F, et al. Brown adipose tissue oxidative metabolism contributes to energy expenditure during acute cold exposure in humans. J Clin Invest. 2012; 122:545–552. [PubMed: 22269323]
14. Muzik O, Mangner TJ, Leonard WR, Kumar A, Janisse J, Granneman JG. 15O PET measurement of blood flow and oxygen consumption in cold-activated human brown fat. J Nucl Med. 2013; 54:523–531. [PubMed: 23362317]
15. Saito M, Okamatsu-ogura Y, Matsushita M, Watanabe K, Yoneshiro T, Nio-kobayashi J, et al. High Incidence of Metabolically Active Brown Adipose Effects of Cold Exposure and Adiposity. Diabetes. 2009; 58:1526–1531. [PubMed: 19401428]
16. Bartelt A, Bruns OT, Reimer R, Hohenberg H, Ittrich H, Peldschus K, et al. Brown adipose tissue activity controls triglyceride clearance. Nat Med. 2011; 17:200–205. [PubMed: 21258337]
17. Tseng Y-H, Cypess AM, Kahn CR. Cellular bioenergetics as a target for obesity therapy. Nat Rev Drug Discov. 2010; 9:465–482. [PubMed: 20514071]

18. Chen M-H, Tong Q. An update on the regulation of adipogenesis. Drug Discov Today Dis Mech. 2013; 10:e15–e19.
19. Stanford KI, Middelbeek RJW, Townsend KL, An D, Nygaard EB, Hitchcox KM, et al. Brown adipose tissue regulates glucose homeostasis and insulin sensitivity. 2013; 123:215–223.
20. Cohen P, Levy JD, Zhang Y, Frontini A, Kolodin DP, Svensson KJ, et al. Ablation of PRDM16 and beige adipose causes metabolic dysfunction and a subcutaneous to visceral fat switch. Cell. 2014; 156:304–316. [PubMed: 24439384]
21. Jo J, Gavrilova O, Pack S, Jou W, Mullen S, Sumner AE, et al. Hypertrophy and/or Hyperplasia: Dynamics of Adipose Tissue Growth. PLoS Comput Biol. 2009; 5:e1000324. [PubMed: 19325873]
22. Schulz TJ, Tseng Y-H. Emerging role of bone morphogenetic proteins in adipogenesis and energy metabolism. Cytokine Growth Factor Rev. 2009; 20:523–531. [PubMed: 19896888]
23. Bauer-Kreisel P, Goepferich A, Blunk T. Cell-delivery therapeutics for adipose tissue regeneration. Adv Drug Deliv Rev. 2010; 62:798–813. [PubMed: 20394786]
24. Townsend KL, Tseng Y. Brown Adipose Tissue: Recent insights into development, metabolic function and therapeutic potential. Adipocyte. 2012; 1:13–24. [PubMed: 23700507]
25. Ahfeldt T, Schinzel RT, Lee Y-K, Hendrickson D, Kaplan A, Lum DH, et al. Programming human pluripotent stem cells into white and brown adipocytes. Nat Cell Biol. 2012; 14:209–219. [PubMed: 22246346]
26. Rodeheffer MS, Birsoy K, Friedman JM. Identification of white adipocyte progenitor cells in vivo. Cell. 2008; 135:240–249. [PubMed: 18835024]
27. Tang W, Zeve D, Suh JM, Bosnakovski D, Kyba M, Hammer RE, et al. White fat progenitor cells reside in the adipose vasculature. Science. 2008; 322:583–586. [PubMed: 18801968]
28. Zhang H, Schulz TJ, Espinoza DO, Huang TL, Emanuelli B, Kristiansen K, et al. Cross talk between insulin and bone morphogenetic protein signaling systems in brown adipogenesis. Mol Cell Biol. 2010; 30:4224–4233. [PubMed: 20584981]
29. Kajimura S, Seale P, Kubota K, Lunsford E, Frangioni JV, Gygi SP, et al. Initiation of myoblast to brown fat switch by a PRDM16-C/EBP-beta transcriptional complex. Nature. 2009; 460:1154–1158. [PubMed: 19641492]
30. Cannon B, Nedergaard J. Brown adipose tissue: function and physiological significance. Physiol Rev. 2004; 84:277–359. [PubMed: 14715917]
31. Cannon B, Nedergaard J. Developmental biology: Neither fat nor flesh. Nature. 2008; 454:947–948. [PubMed: 18719573]
32. Seale P, Bjork B, Yang W, Kajimura S, Chin S, Kuang S, et al. PRDM16 controls a brown fat/skeletal muscle switch. Nature. 2008; 454:961–967. [PubMed: 18719582]
33. Schulz TJ, Huang P, Huang TL, Xue R, McDougall LE, Townsend KL, et al. Brown-fat paucity due to impaired BMP signalling induces compensatory browning of white fat. Nature. 2013; 495:379–383. [PubMed: 23485971]
34. Lidell ME, Betz MJ, Dahlqvist Leinhard O, Heglind M, Elander L, Slawik M, et al. Evidence for two types of brown adipose tissue in humans. Nat Med. 2013; 19:631–634. [PubMed: 23603813]
35. Petrovic N, Walden TB, Shabalina IG, Timmons JA, Cannon B, Nedergaard J. Chronic peroxisome proliferator-activated receptor gamma (PPARgamma) activation of epididymally derived white adipocyte cultures reveals a population of thermogenically competent, UCP1-containing adipocytes molecularly distinct from classic brown adipocyt. J Biol Chem. 2010; 285:7153–7164. [PubMed: 20028987]
36. Wu J, Boström P, Sparks LM, Ye L, Choi JH, Giang A-H, et al. Beige adipocytes are a distinct type of thermogenic fat cell in mouse and human. Cell. 2012; 150:366–376. [PubMed: 22796012]
37. Cypess AM, White AP, Vernochet C, Schulz TJ, Xue R, Sass CA, et al. Anatomical localization, gene expression profiling and functional characterization of adult human neck brown fat. Nat Med. 2013; 19:635–640. [PubMed: 23603815]
38. Lee P, Werner CD, Kebebew E, Celi FS. Functional thermogenic beige adipogenesis is inducible in human neck fat. Int J Obes (Lond). 2014; 38:170–176. [PubMed: 23736373]
39. Lee Y-H, Mottillo EP, Granneman JG. Adipose tissue plasticity from WAT to BAT and in between. Biochim Biophys Acta. 2014; 1842:358–369. [PubMed: 23688783]

40. Wang QA, Tao C, Gupta RK, Scherer PE. Tracking adipogenesis during white adipose tissue development, expansion and regeneration. Nat Med. 2013; 19:1338–1344. [PubMed: 23995282]
41. Rosenwald M, Perdikari A, Rülicke T, Wolfrum C. Bi-directional interconversion of brite and white adipocytes. Nat Cell Biol. 2013; 15:659–667. [PubMed: 23624403]
42. Lee Y-H, Petkova AP, Mottillo EP, Granneman JG. In vivo identification of bipotential adipocyte progenitors recruited by β3-adrenoceptor activation and high-fat feeding. Cell Metab. 2012; 15:480–491. [PubMed: 22482730]
43. Lichtenbelt W van M, Kingma B, van der Lans A, Schellen L. Cold exposure - an approach to increasing energy expenditure in humans. Trends Endocrinol Metab. 2014; 25:165–167. [PubMed: 24462079]
44. Boström P, Wu J, Jedrychowski MP, Korde A, Ye L, Lo JC, et al. A PGC1-α-dependent myokine that drives brown-fat-like development of white fat and thermogenesis. Nature. 2012; 481:463–468. [PubMed: 22237023]
45. Gaich G, Chien JY, Fu H, Glass LC, Deeg MA, Holland WL, et al. The effects of LY2405319, an FGF21 analog, in obese human subjects with type 2 diabetes. Cell Metab. 2013; 18:333–340. [PubMed: 24011069]
46. Lee P, Linderman JD, Smith S, Brychta RJ, Wang J, Idelson C, et al. Irisin and FGF21 are cold-induced endocrine activators of brown fat function in humans. Cell Metab. 2014; 19:302–309. [PubMed: 24506871]
47. Zhang Y, Li R, Meng Y, Li S, Donelan W, Zhao Y, et al. Irisin stimulates browning of white adipocytes through mitogen-activated protein kinase p38 MAP kinase and ERK MAP kinase signaling. Diabetes. 2014; 63:514–525. [PubMed: 24150604]
48. Sun L, Xie H, Mori MA, Alexander R, Yuan B, Hattangadi SM, et al. Mir193b-365 is essential for brown fat differentiation. Nat Cell Biol. 2011; 13:958–965. [PubMed: 21743466]
49. Mori M, Nakagami H, Rodriguez-Araujo G, Nimura K, Kaneda Y. Essential role for miR-196a in brown adipogenesis of white fat progenitor cells. PLoS Biol. 2012; 10:e1001314. [PubMed: 22545021]
50. Trajkovski M, Ahmed K, Esau CC, Stoffel M. MyomiR-133 regulates brown fat differentiation through Prdm16. Nat Cell Biol. 2012; 14:1330–1335. [PubMed: 23143398]
51. Trajkovski M, Lodish H. MicroRNA networks regulate development of brown adipocytes. Trends Endocrinol Metab. 2013; 24:442–450. [PubMed: 23809233]
52. Chen Y, Siegel F, Kipschull S, Haas B, Fröhlich H, Meister G, et al. miR-155 regulates differentiation of brown and beige adipocytes via a bistable circuit. Nat Commun. 2013; 4:1769. [PubMed: 23612310]
53. Liu W, Kuang S. miR-133 links to energy balance through targeting Prdm16. J Mol Cell Biol. 2013; 5:432–434. [PubMed: 24085747]
54. Sun L, Trajkovski M. MiR-27 orchestrates the transcriptional regulation of brown adipogenesis. Metabolism. 2014; 63:272–282. [PubMed: 24238035]
55. Nedergaard J, Cannon B. How brown is brown fat? It depends where you look. Nat Med. 2013; 19:540–541. [PubMed: 23652104]
56. Lowell BB, S-Susulic V, Hamann A, Lawitts JA, Himms-Hagen J, Boyer BB, et al. Development of obesity in transgenic mice after genetic ablation of brown adipose tissue. Nature. 1993; 366:740–742. [PubMed: 8264795]
57. Mohsen-Kanson T, Hafner AL, Wdziekonski B, Takashima Y, Villageois P, Carrière A, et al. Differentiation of human induced pluripotent stem cells into brown and white adipocytes: Role of Pax3. Stem Cells. 2014; 32:1459–1467. [PubMed: 24302443]
58. Lee, Y-K.; Cowan, CA. Methods Enzymol. 1st ed.. Vol. 538. Elsevier Inc.; 2014. Differentiation of white and brown adipocytes from human pluripotent stem cells; p. 35-47.
59. Martin GR. Isolation of a pluripotent cell line from early mouse embryos cultured in medium conditioned by teratocarcinoma stem cells. Proc Natl Acad Sci U S A. 1981; 78:7634–7638. [PubMed: 6950406]
60. Risau W, Sariola H, Zerwes HG, Sasse J, Ekblom P, Kemler R, et al. Vasculogenesis and angiogenesis in embryonic-stem-cell-derived embryoid bodies. Development. 1988; 102:471–478. [PubMed: 2460305]

61. Reubinoff BE, Pera MF, Fong CY, Trounson A, Bongso A. Embryonic stem cell lines from human blastocysts: somatic differentiation in vitro. Nat Biotechnol. 2000; 18:399–404. [PubMed: 10748519]
62. Taura D, Noguchi M, Sone M, Hosoda K, Mori E, Okada Y, et al. Adipogenic differentiation of human induced pluripotent stem cells: comparison with that of human embryonic stem cells. FEBS Lett. 2009; 583:1029–1033. [PubMed: 19250937]
63. Nishio M, Yoneshiro T, Nakahara M, Suzuki S, Saeki K, Hasegawa M, et al. Production of functional classical brown adipocytes from human pluripotent stem cells using specific hemopoietin cocktail without gene transfer. Cell Metab. 2012; 16:394–406. [PubMed: 22958922]
64. Noguchi M, Hosoda K, Nakane M, Mori E, Nakao K, Taura D, et al. In Vitro Characterization and Engraftment of Adipocytes Derived from Human Induced Pluripotent Stem Cells and Embryonic Stem Cells. Stem Cells Dev. 2013; 22:1–11. [PubMed: 23013234]
65. Nishio M, Saeki K. Differentiation of human pluripotent stem cells into highly functional classical brown adipocytes. Methods Enzymol. 2014; 537:177–197. [PubMed: 24480347]
66. Kang X, Xie Y, Powell HM, James Lee L, Belury MA, Lannutti JJ, et al. Adipogenesis of murine embryonic stem cells in a three-dimensional culture system using electrospun polymer scaffolds. Biomaterials. 2007; 28:450–458. [PubMed: 16997371]
67. Hoshino K. Transplantability of mammary gland in brown fat pads of mice. Nature. 1967; 213:194–195. [PubMed: 6030585]
68. Tanzi MC, Farè S. Adipose tissue engineering: state of the art, recent advances and innovative approaches. Expert Rev Med Devices. 2009; 6:533–551. [PubMed: 19751125]
69. Patrick CW. Adipose tissue engineering: the future of breast and soft tissue reconstruction following tumor resection. Semin Surg Oncol. 19:302–311. n.d. [PubMed: 11135487]
70. Orive G, Hernández RM, Gascón AR, Calafiore R, Chang TMS, De Vos P, et al. Cell encapsulation: promise and progress. Nat Med. 2003; 9:104–107. [PubMed: 12514721]
71. Wang W, Liu X, Xie Y, Zhang H, Yu W, Xiong Y, et al. Microencapsulation using natural polysaccharides for drug delivery and cell implantation. J Mater Chem. 2006; 16:3252.
72. Slaughter BV, Khurshid SS, Fisher OZ, Khademhosseini A, Peppas NA. Hydrogels in regenerative medicine. Adv Mater. 2009; 21:3307–3329. [PubMed: 20882499]
73. Sun J, Tan H. Alginate-based biomaterials for regenerative medicine applications. Materials (Basel). 2013; 6:1285–1309.
74. Jun Y, Kim MJ, Hwang YH, Jeon EA, Kang AR, Lee S-H, et al. Microfluidics-generated pancreatic islet microfibers for enhanced immunoprotection. Biomaterials. 2013; 34:8122–8130. [PubMed: 23927952]
75. Raof NA, Padgen MR, Gracias AR, Bergkvist M, Xie Y. One-dimensional self-assembly of mouse embryonic stem cells using an array of hydrogel microstrands. Biomaterials. 2011; 32:4498–4505. [PubMed: 21459438]
76. Lu HF, Narayanan K, Lim S-X, Gao S, Leong MF, Wan ACa. A 3D microfibrous scaffold for long-term human pluripotent stem cell self-renewal under chemically defined conditions. Biomaterials. 2012; 33:2419–2430. [PubMed: 22196900]
77. Onoe H, Okitsu T, Itou A, Kato-Negishi M, Gojo R, Kiriya D, et al. Metre-long cell-laden microfibres exhibit tissue morphologies and functions. Nat Mater. 2013; 12:584–590. [PubMed: 23542870]
78. Zhang X, Qin J. Modified alginate/chitosan hollow microfiber as a biocompatible frame for blood vessel reconstruction. Nano Life. 2012; 02 121009023900001.
79. Takei T, Kishihara N, Sakai S, Kawakami K. Novel technique to control inner and outer diameter of calcium-alginate hydrogel hollow microfibers, and immobilization of mammalian cells. Biochem Eng J. 2010; 49:143–147.
80. Lee BR, Lee KH, Kang E, Kim D-S, Lee S-H. Microfluidic wet spinning of chitosan-alginate microfibers and encapsulation of HepG2 cells in fibers. Biomicrofluidics. 2011; 5:22208. [PubMed: 21799714]
81. Akbari M, Tamayol A, Laforte V, Annabi N, Najafabadi AH, Khademhosseini A, et al. Composite living fibers for creating tissue constructs using textile techniques. Adv Funct Mater. 2014; 24:4060–4067. [PubMed: 25411576]

82. Robertson E, Bradley A, Kuehn M, Evans M. Germ-line transmission of genes introduced into cultured pluripotential cells by retroviral vector. Nature. 323:445–448. n.d. [PubMed: 3762693]

83. Keller G, Kennedy M, Papayannopoulou T, Wiles M. Hematopoietic commitment during embryonic stem cell differentiation in culture. Mol Cell Biol. 1993; 13:473–486. [PubMed: 8417345]

84. Fasshauer M, Klein J, Kriauciunas KM, Ueki K, Benito M, Kahn CR. Essential role of insulin receptor substrate 1 in differentiation of brown adipocytes. Mol Cell Biol. 2001; 21:319–329. [PubMed: 11113206]

85. Fasshauer M, Klein J, Ueki K, Kriauciunas KM, Benito M, White MF, et al. Essential role of insulin receptor substrate-2 in insulin stimulation of Glut4 translocation and glucose uptake in brown adipocytes. J Biol Chem. 2000; 275:25494–25501. [PubMed: 10829031]

86. Colton CK. Implantable biohybrid artificial organs. Cell Transplant. 1995; 4:415–436. [PubMed: 7582573]

87. Griffith CK, Miller C, Sainson RCA, Calvert JW, Jeon NL, Hughes CCW, et al. Diffusion limits of an in vitro thick prevascularized tissue. Tissue Eng. 11:257–266. n.d. [PubMed: 15738680]

88. Tseng Y-H, Kokkotou E, Schulz TJ, Huang TL, Winnay JN, Taniguchi CM, et al. New role of bone morphogenetic protein 7 in brown adipogenesis and energy expenditure. Nature. 2008; 454:1000–1004. [PubMed: 18719589]

89. Pountos I, Georgouli T, Henshaw K, Bird H, Jones E, Giannoudis P V. The effect of bone morphogenetic protein-2, bone morphogenetic protein-7, parathyroid hormone, and platelet-derived growth factor on the proliferation and osteogenic differentiation of mesenchymal stem cells derived from osteoporotic bone. J Orthop Trauma. 2010; 24:552–556. [PubMed: 20736793]

90. Zhi L, Chen C, Pang X, Uludag H, Jiang H. Synergistic effect of recombinant human bone morphogenic protein-7 and osteogenic differentiation medium on human bone-marrow-derived mesenchymal stem cells in vitro. Int Orthop. 2011; 35:1889–1895. [PubMed: 21487672]

91. Kim HK, Kim JH, Park DS, Park KS, Kang SS, Lee JS, et al. Osteogenesis induced by a bone forming peptide from the prodomain region of BMP-7. Biomaterials. 2012; 33:7057–7063. [PubMed: 22795855]

92. Sell H, Deshaies Y, Richard D. The brown adipocyte: update on its metabolic role. Int J Biochem Cell Biol. 2004; 36:2098–2104. [PubMed: 15313455]

93. Wu Z, Satterfield MC, Bazer FW, Wu G. Regulation of brown adipose tissue development and white fat reduction by L-arginine. Curr Opin Clin Nutr Metab Care. 2012; 15:529–538. [PubMed: 23075933]

94. Lee P, Swarbrick MM, Ho KKY. Brown adipose tissue in adult humans: a metabolic renaissance. Endocr Rev. 2013; 34:413–438. [PubMed: 23550082]

95. Greenwood-Goodwin M, Teasley ES, Heilshorn SC. Dual-stage growth factor release within 3D protein-engineered hydrogel niches promotes adipogenesis. Biomater Sci. 2014; 2:1627–1639. [PubMed: 25309741]

96. Yao R, Zhang R, Lin F, Luan J. Injectable cell/hydrogel microspheres induce the formation of fat lobule-like microtissues and vascularized adipose tissue regeneration. Biofabrication. 2012; 4:045003. [PubMed: 23075755]

97. Wang N, Adams G, Buttery L, Falcone FH, Stolnik S. Alginate encapsulation technology supports embryonic stem cells differentiation into insulin-producing cells. J Biotechnol. 2009; 144:304–312. [PubMed: 19686786]

98. Maguire T, Novik E, Schloss R, Yarmush M. Alginate-PLL microencapsulation: Effect on the differentiation of embryonic stem cells into hepatocytes. Biotechnol Bioeng. 2006; 93:581–591. [PubMed: 16345081]

99. Raof NA, Raja WK, Castracane J, Xie Y. Bioengineering embryonic stem cell microenvironments for exploring inhibitory effects on metastatic breast cancer cells. Biomaterials. 2011; 32:4130–4139. [PubMed: 21411140]

100. Liu J, Zhou H, Weir MD, Xu HHK, Chen Q, Trotman CA. Fast-Degradable Microbeads Encapsulating Human Umbilical Cord Stem Cells in Alginate. 2012; 18

101. Huang X, Zhang X, Wang X, Wang C, Tang B. Microenvironment of alginate-based microcapsules for cell culture and tissue engineering. J Biosci Bioeng. 2012; 114:1–8. [PubMed: 22561878]
102. Yao R, Zhang R, Luan J, Lin F. Alginate and alginate/gelatin microspheres for human adipose-derived stem cell encapsulation and differentiation. Biofabrication. 2012; 4:025007. [PubMed: 22556122]
103. Olderøy MO, Xie M, Andreassen J-P, Strand BL, Zhang Z, Sikorski P. Viscoelastic properties of mineralized alginate hydrogel beads. J Mater Sci Mater Med. 2012; 23:1619–1627. [PubMed: 22552827]
104. Takei T, Kitazono J, Tanaka S, Nishimata H, Yoshida M. Necrotic regions are absent in fiber-shaped cell aggregates, approximately 100 μm in diameter. Artif Cells, Nanomedicine, Biotechnol. 2014:1–4.
105. Neal D, Sakar MS, Ong L-LS, Harry Asada H. Formation of elongated fascicle-inspired 3D tissues consisting of high-density, aligned cells using sacrificial outer molding. Lab Chip. 2014; 14:1907–1916. [PubMed: 24744046]
106. Hsiao AY, Okitsu T, Onoe H, Kiyosawa M, Teramae H, Iwanaga S, et al. Smooth Muscle-Like Tissue Constructs with Circumferentially Oriented Cells Formed by the Cell Fiber Technology. PLoS One. 2015; 10:e0119010. [PubMed: 25734774]
107. Shin S-J, Park J-Y, Lee J-Y, Park H, Park Y-D, Lee K-B, et al. "On the fly" continuous generation of alginate fibers using a microfluidic device. Langmuir. 2007; 23:9104–9108. [PubMed: 17637008]
108. Sugiura S, Oda T, Aoyagi Y, Satake M, Ohkohchi N, Nakajima M. Tubular gel fabrication and cell encapsulation in laminar flow stream formed by microfabricated nozzle array. Lab Chip. 2008; 8:1255–1257. [PubMed: 18651064]
109. Hu M, Deng R, Schumacher KM, Kurisawa M, Ye H, Purnamawati K, et al. Hydrodynamic spinning of hydrogel fibers. Biomaterials. 2010; 31:863–869. [PubMed: 19878994]
110. Zhang S, Greenfield MA, Mata A, Palmer LC, Bitton R, Mantei JR, et al. A self-assembly pathway to aligned monodomain gels. Nat Mater. 2010; 9:594–601. [PubMed: 20543836]
111. Kang E, Jeong GS, Choi YY, Lee KH, Khademhosseini A, Lee S-H. Digitally tunable physicochemical coding of material composition and topography in continuous microfibres. Nat Mater. 2011; 10:877–883. [PubMed: 21892177]
112. Yamada M, Sugaya S, Naganuma Y, Seki M. Microfluidic synthesis of chemically and physically anisotropic hydrogel microfibers for guided cell growth and networking. Soft Matter. 2012; 8:3122.
113. Phillips B. Differentiation of embryonic stem cells for pharmacological studies on adipose cells. Pharmacol Res. 2003; 47:263–268. [PubMed: 12644382]
114. Dani C, Smith AG, Dessolin S, Leroy P, Staccini L, Villageois P, et al. Differentiation of embryonic stem cells into adipocytes in vitro. J Cell Sci. 1997; 110:1279–1285. [PubMed: 9202388]
115. Okada Y, Shimazaki T, Sobue G, Okano H. Retinoic-acid-concentration-dependent acquisition of neural cell identity during in vitro differentiation of mouse embryonic stem cells. Dev Biol. 2004; 275:124–142. [PubMed: 15464577]
116. Rosen ED, Sarraf P, Troy AE, Bradwin G, Moore K, Milstone DS, et al. PPAR gamma is required for the differentiation of adipose tissue in vivo and in vitro. Mol Cell. 1999; 4:611–617. [PubMed: 10549292]
117. Géloën, a; Trayhurn, P. Regulation of the level of uncoupling protein in brown adipose tissue by insulin requires the mediation of the sympathetic nervous system. FEBS Lett. 1990; 267:265–267. [PubMed: 2199218]
118. Golozoubova V, Hohtola E, Matthias A, Jacobsson A, Cannon B, Nedergaard J. Only UCP1 can mediate adaptive nonshivering thermogenesis in the cold. J Fed Am Soc Exp Biol. 2001; 15:2048–2050. [PubMed: 11511509]
119. Pittenger MF, Mackay aM, Beck SC, Jaiswal RK, Douglas R, Mosca JD, et al. Multilineage potential of adult human mesenchymal stem cells. Science. 1999; 284:143–147. [PubMed: 10102814]

120. Lu Z, Roohani-Esfahani S-I, Wang G, Zreiqat H. Bone biomimetic microenvironment induces osteogenic differentiation of adipose tissue-derived mesenchymal stem cells. Nanomedicine. 2012; 8:507–515. [PubMed: 21839050]

121. Bidarra SJ, Barrias CC, Fonseca KB, Barbosa MA, Soares RA, Granja PL. Injectable in situ crosslinkable RGD-modified alginate matrix for endothelial cells delivery. Biomaterials. 2011; 32:7897–7904. [PubMed: 21784515]

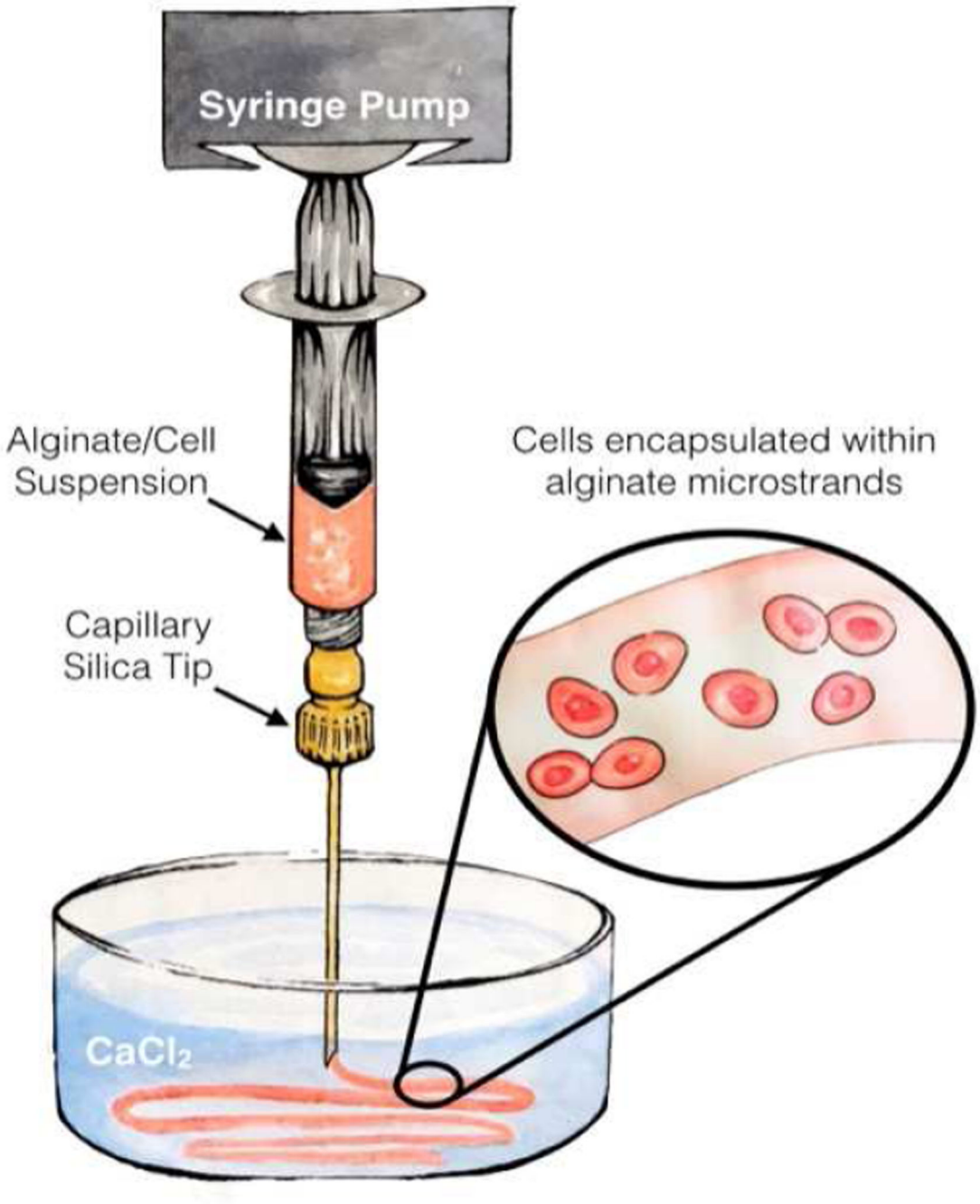

Figure 1.
Scheme of microfluidic synthesis of an alginate hydrogel microstrand for cell encapsulation.

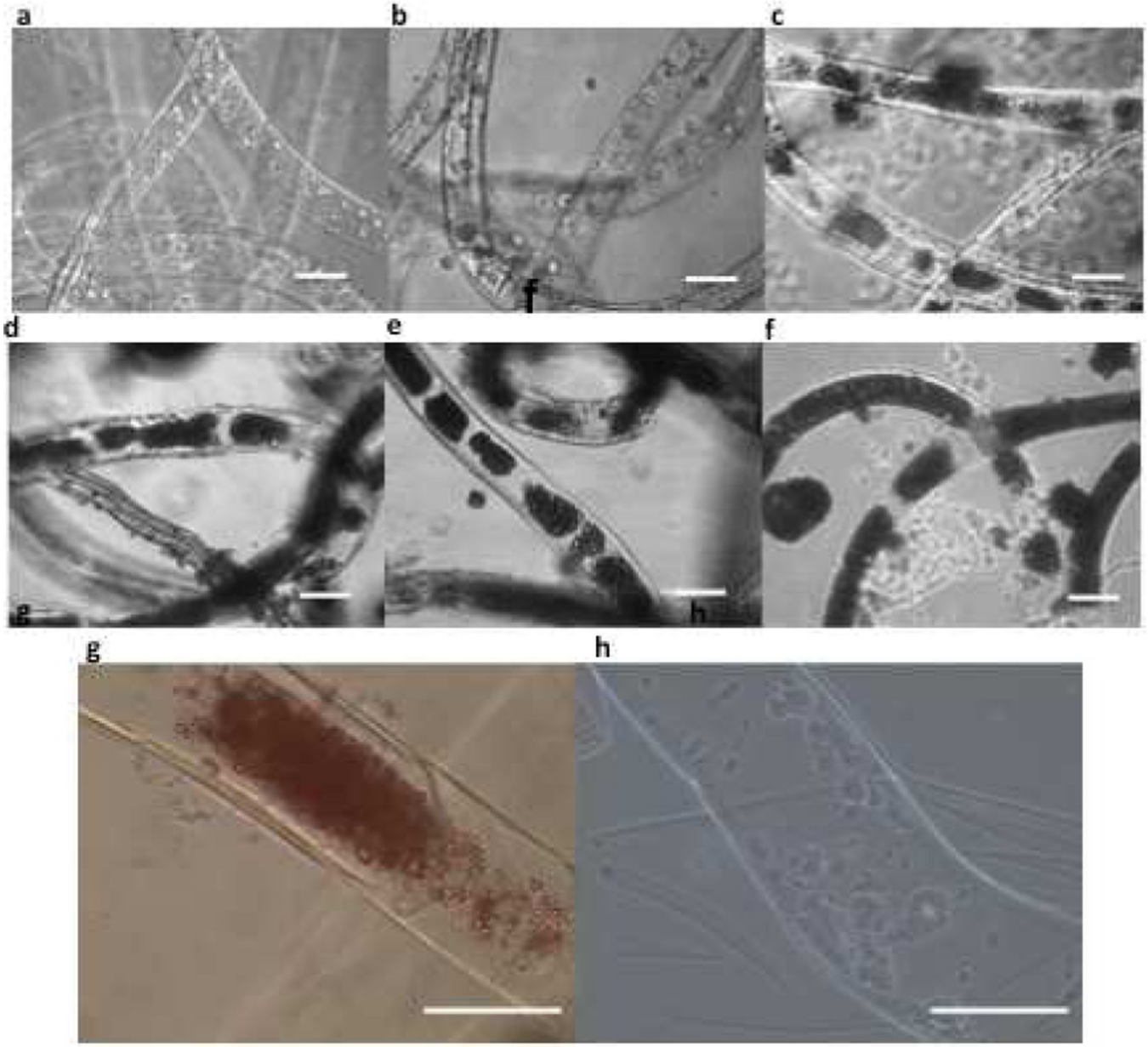

Figure 2.

Time course of cell growth and brown adipogenesis of WT-1 preadipocytes encapsulated within alginate hydrogel microstrands: Day 2 (a), Day 5 (b), Day 8 (c), Day 11 (d), Day 15 (e), and Day 20 (f). At day 20, the formation of lipid droplets in adipocytes was confirmed by oil red O staining of cells (g) in the differentiated WT-1 cells in hydrogel microstrands, compared to (h) the control of cells without adipogenesis induction. Scale bar = 100 μm.

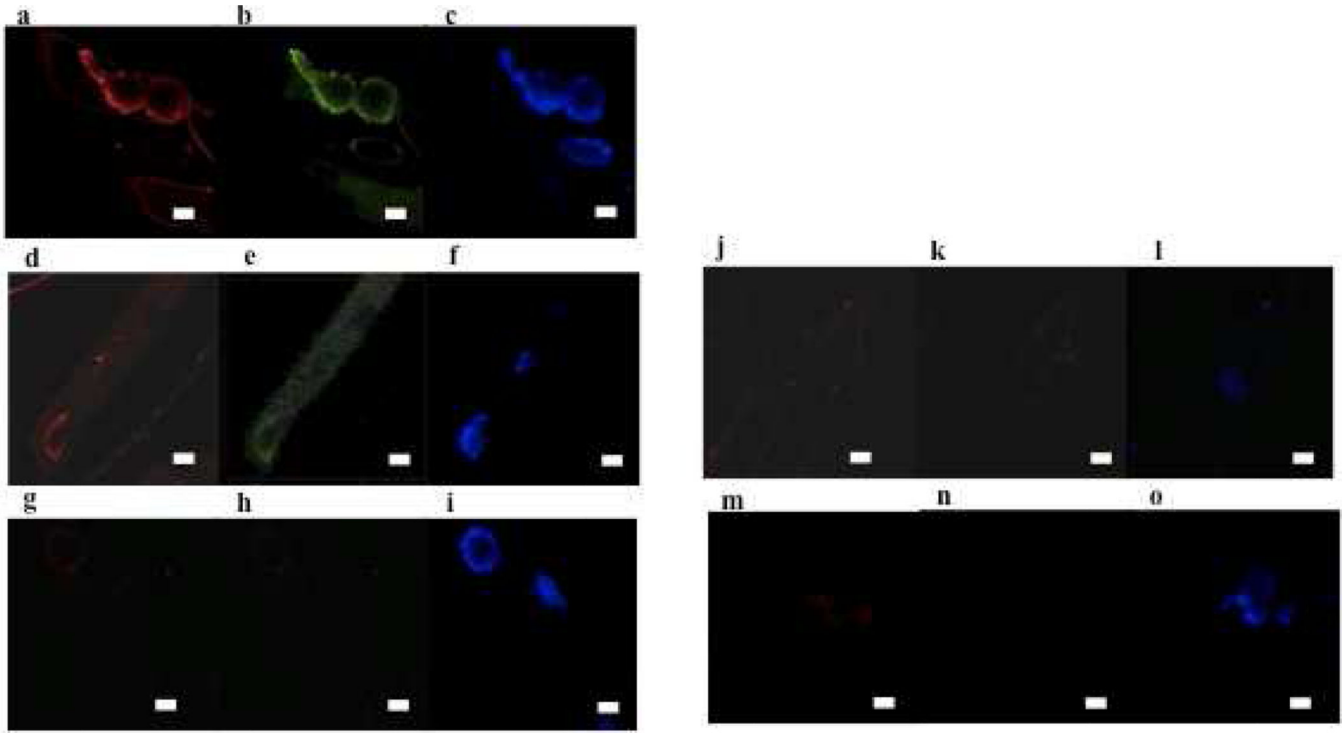

Figure 3.

Confocal images of differentiated WT-1 cells in alginate microstrands on day 15. Terminally differentiated brown adipocytes (a–f) and undifferentiated control of brown preadipocytes in alginate microstrands without the addition of induction or differentiation media (i–o). Expression of PPARγ2 (a and j). Perilipin (b,e,k, and n). UCP1 (d and m). and (c, f, i, l, and o) DAPI for both conditions. Negative controls with secondary antibody Alexa Fluor® 488 only (g) and secondary antibody Alexa Fluor® 647 only (h). Scale bar = 100 μm.

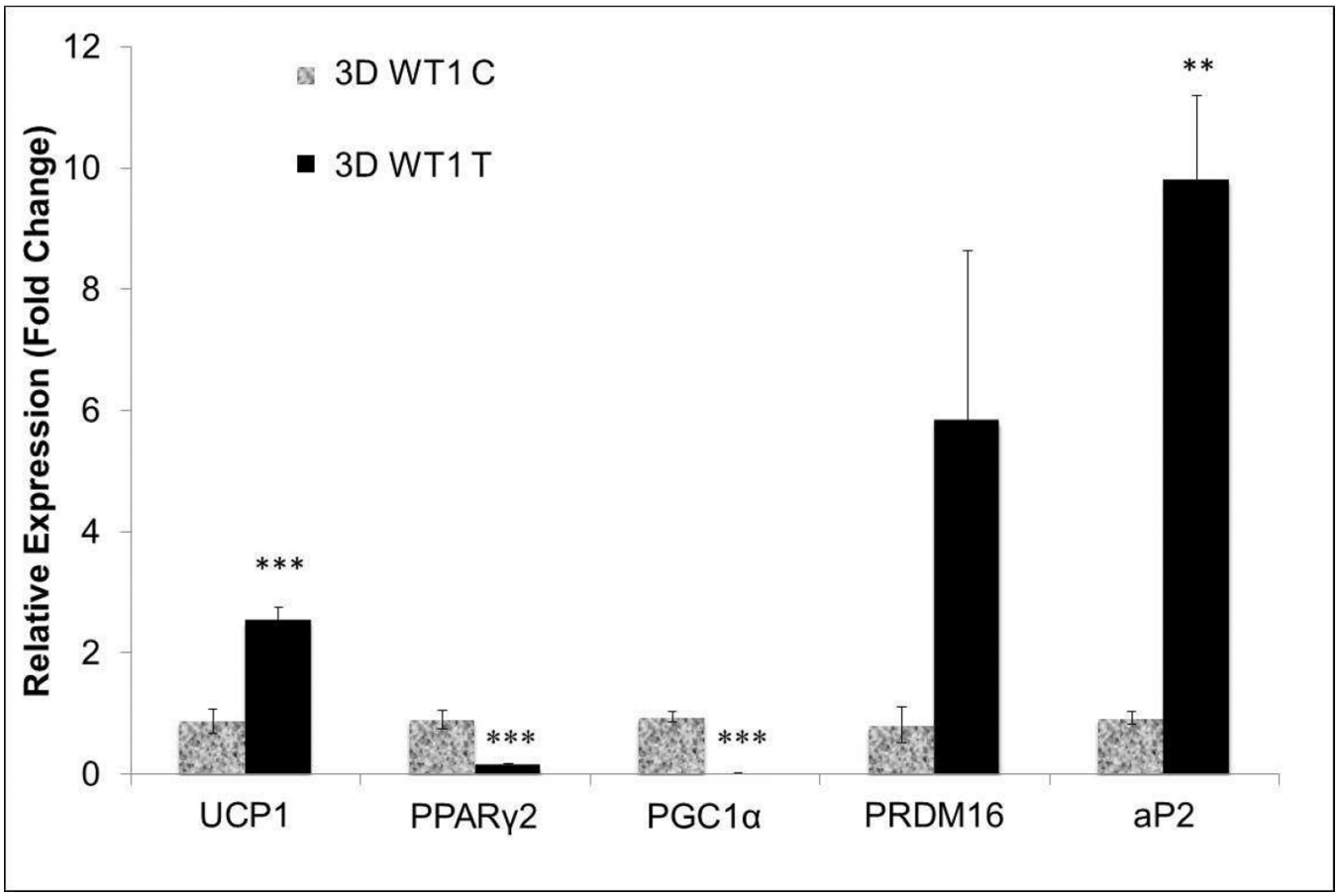

Figure 4.

qPCR analysis of gene expression of terminally differentiated WT-1 brown adipocytes in 3D alginate hydrogel microstrands (3D WT1 T) compared to WT-1 cells grown in 3D without brown adipogensis induction (3D WT1 C). * $p<0.05$, ** $p<0.005$, *** $p<0.001$.

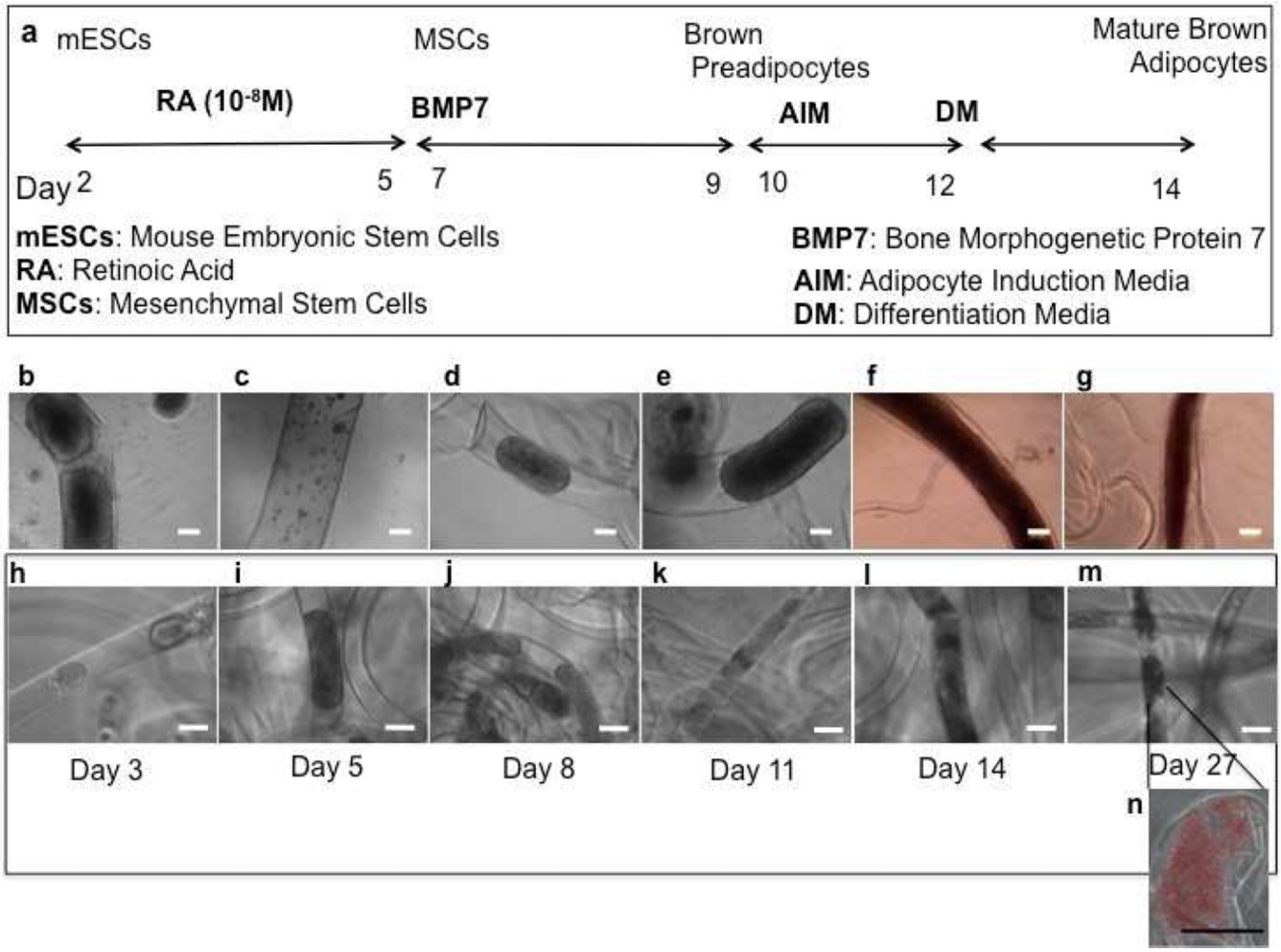

Figure 5.

Differentiation scheme for CCE ES cells in microstrands timeline (a), determination of optimal brown adipogenesis differentiation of CCE ES cells within alginate hyrogel microstrands in terms of liquid and gel interior (b and c), 100 or 250 μm inner diameter (d and e), and oil red O staining for 3.3 or 8.3 nM BMP 7 (f and g). Complete time course using these conditions is also represented (h–m) along with oil red O staining at day 27 (n). Scale bar = 100 μm.

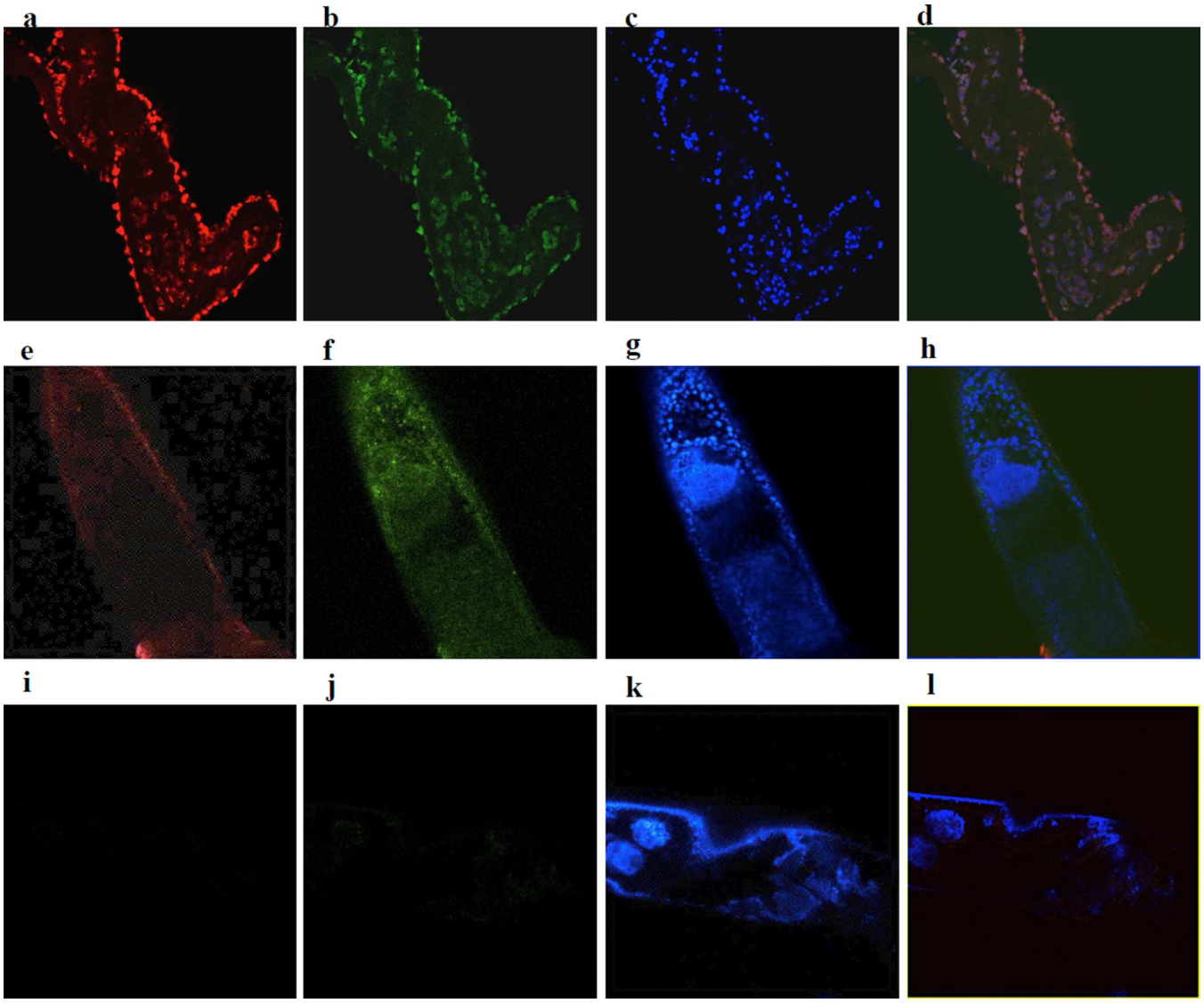

Figure 6.

Confocal images of ESC-derived brown adipocytes in alginate hydrogel microstrands, confirming expression of PPARγ2 (a), Perilipin (b and e), brown adipocyte-defining UCP1 (d), co-stained with DAPI (c,f, and i), and merged (d,h, and l). Negative controls were also imaged for each wavelength in order to eliminate the chance of background signal (g and h). Scale bar = 100 μm.

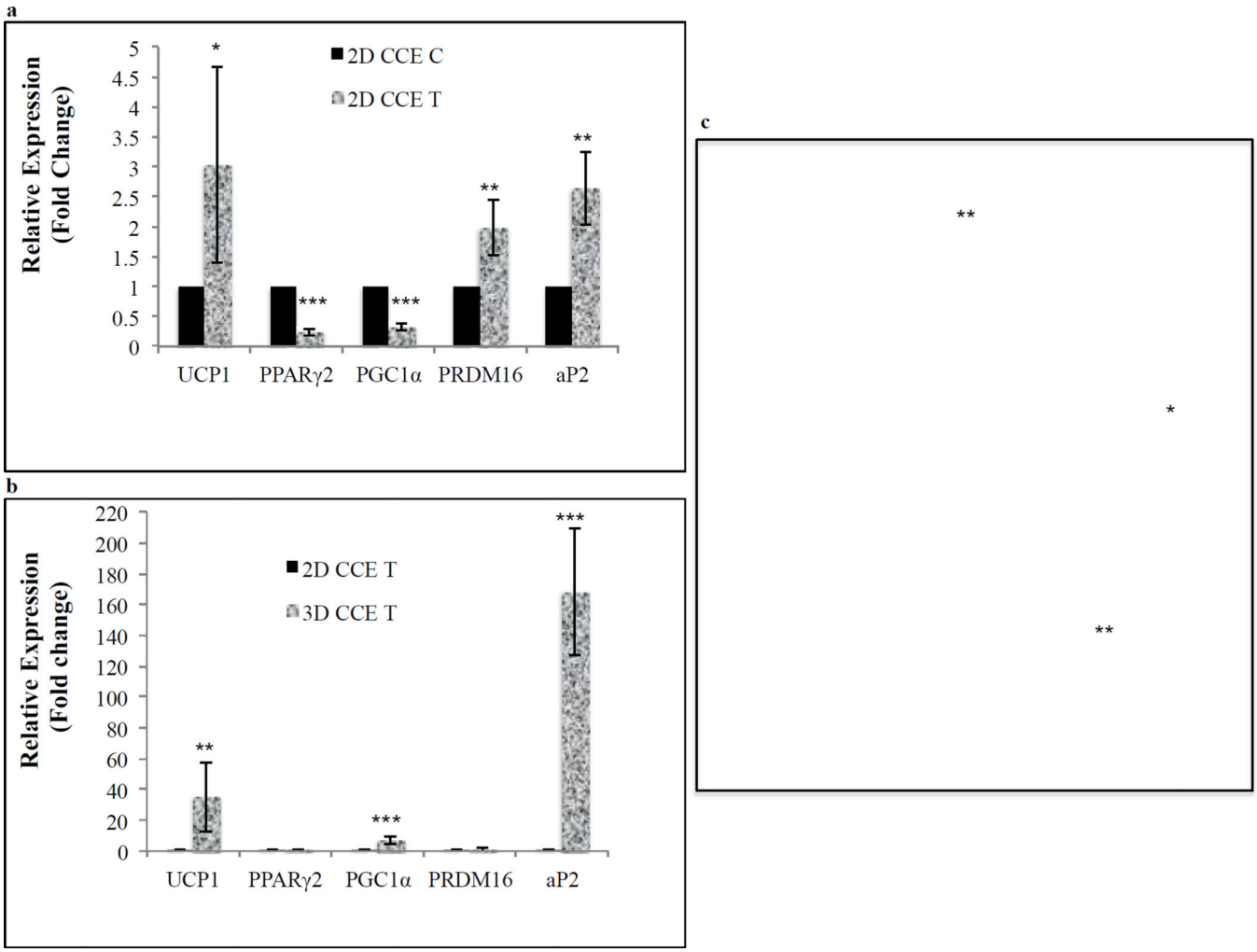

Figure 7.

qPCR analysis of gene expression of brown adipogenic ESCs grown in 2D and 3D. (a) 2D ESC-differentiated brown adipocytes (2D CCE T) exhibited significantly higher gene expression of brown adipocyte-defining UCP1 and adipocyte marker PRDM16 and aP2 than 2D undifferentiated long-term culture (2D CCE C). (b) Comparison of ESC-differentiated brown adipocytes grown in 3D (3D CCE T) to 2D (2D CCE T). (c) Comparison of 2D undifferentiated long-term culture (2D CCE C) (c) to CCE cells grown for 2 days (2D CCE Day 2). * $p<0.05$, ** $p<0.005$, *** $p<0.001$.

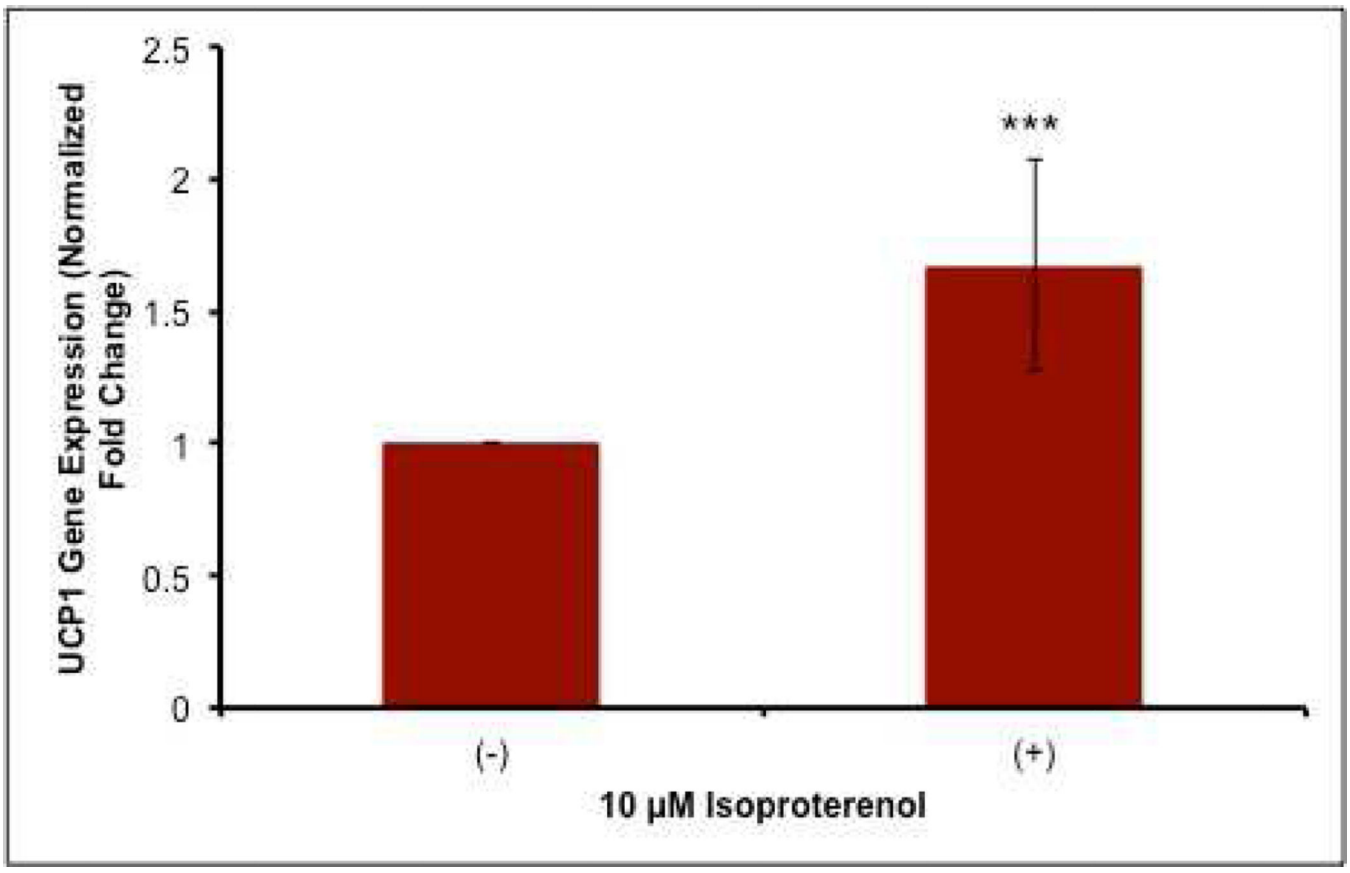

Figure 8.

qPCR gene expression of brown adipocyte-defining UCP1 in 3D ESC-differentiated brown adipocytes with (+) and without (−) isoproterenol treatment. *** $p<0.001$.

Table 1

qPCR analysis of gene expression of brown adipocyte markers in mouse CCE ESCs grown in 3D alginate hydrogel microstrands compared to untreated control (n=3).

	3D CCE C	3D CCE T
UCP-1	Undetermined*	30.4 ± 0.3
PPARγ2	26.2 ± 2.2	26.7 ± 2.0
PGC1α	Undetermined*	30.6 ± 0.3
PRDM-16	Undetermined*	30.1 ± 1.6
aP2	30.2 ± 0.3	21.8 ± 0.2
ARBP	22.7 ± 0.7	19.0 ± 0.0

* Denote expression that was too low to be detected.

** Show cycle threshold values for qPCR, in which the lower the cycle threshold, the higher the gene of interest is expressed in the sample.